

Strategies for measurement-based quantum computation with cluster states transformed by stochastic local operations and classical communication

Adam G. D'Souza and David L. Feder

*Department of Physics and Astronomy and Institute for Quantum Information Science,
University of Calgary, Calgary, Alberta, Canada*

(Dated: November 2, 2018)

We examine cluster states transformed by stochastic local operations and classical communication, as a resource for deterministic universal computation driven strictly by projective measurements. We identify circumstances under which such states in one dimension constitute resources for random-length single-qubit rotations, in one case quasi-deterministically ($N-U-N$ states) and in another probabilistically ($B-U-B$ states). In contrast to the cluster states, the $N-U-N$ states exhibit spin correlation functions that decay exponentially with distance, while the $B-U-B$ states can be arbitrarily locally pure. A two-dimensional square $N-U-N$ lattice is a universal resource for quasi-deterministic measurement-based quantum computation. Measurements on cubic $B-U-B$ states yield two-dimensional cluster states with bond defects, whose connectivity exceeds the percolation threshold for a critical value of the local purity.

I. INTRODUCTION

In the Measurement-Based Quantum Computation (MBQC) model [1, 2], one starts with a highly entangled many-qubit quantum state called a resource state, and processes logical information via single-qubit measurements on the physical qubits of the resource state. In order to compensate for the randomness of the measurement outcomes, the bases in which measurements are performed must be conditioned on the outcomes of previous measurements. Proceeding in this way, one can teleport logical quantum information situated on one part of the state to another part, but having been subjected to some desired unitary transformation. If the basic unitary transformations that can be applied via single-qubit measurements on the resource state generate a set that is dense in $SU(2)$, then the resource is said to be universal (in the terminology of Ref. [3], this is the notion of CQ-universality, and such a resource state would be called a universal state preparator).

The archetypal family of resource states known to be universal for efficient MBQC is the so-called cluster state [1, 2]. This state is special in several ways: all spin correlation functions are strictly nearest-neighbor [4, 5], the localizable entanglement between any pair of qubits is maximal [4, 5], it is the only state (up to local unitaries) on small system sizes that saturates the Tsallis and Renyi entropies of entanglement [6], it cannot be the non-degenerate ground state of a two-body spin Hamiltonian [7, 8], and so on. One might expect that one or more of these properties would be necessarily satisfied by any universal resource state. This has turned out not to be the case; several authors in recent years have identified resources that differ materially from the cluster states [4, 5, 9–14].

The newly discovered richness in the landscape of resources notwithstanding, the property of universality is exceedingly rare; not only must a family of universal resource states saturate various measures of entanglement in the thermodynamic limit [3, 15], but the entangle-

ment with respect to other measures must not be too high [16, 17]. Therefore, it is highly unlikely that a random pure state will be universal, so a search for new resources must be heavily constrained in order to have a reasonable chance of success.

Recently, a number of new resources [4, 5, 10, 18] have been proven to be universal by means of reduction to a known resource state [19]. The reduction strategies of interest are those composed purely of local operations, possibly augmented by classical communication. They are typically stochastic, in the sense that the known resource state is smaller than the original state. In other words, these resources all appear to be within the equivalence class of the cluster states under Stochastic Local Operations and Classical Communication (SLOCC). The SLOCC-equivalence class of an n -qubit pure state is known to be its orbit under $GL(2, \mathbb{C})^{\otimes n}$, the group of n -fold tensor products of two-by-two invertible matrices over the complex numbers. In other words, two n -qubit states $|\psi\rangle$ and $|\phi\rangle$ are equivalent under SLOCC if and only if

$$|\psi\rangle = S^{(1)} \otimes S_2 \otimes \cdots \otimes S_n |\phi\rangle \quad (1)$$

where the $\{S_i\} \in GL(2, \mathbb{C})$ are invertible, two-by-two complex matrices.

A natural question thus arises: are all universal MBQC resources SLOCC-equivalent to the cluster states? More precisely, is any n -qubit element of a family of universal resource states SLOCC-equivalent to an n -qubit cluster state?

In this paper, we tackle a related question, namely: what states in the SLOCC-equivalence class of the two-dimensional cluster states are universal for MBQC? It is clear, by construction, that each state in this class can be stochastically reduced to a cluster state, but what is not clear is whether it is possible to compute directly on the image of a cluster state under some invertible, local map. We show that there is a restricted subclass of invertible local transformations, strictly including the local unitaries, whose image is a set of quasi-deterministic

resources for MBQC, where in general the computation is of random length and ‘repeat-until-success’ strategies must be employed (c.f. Refs. [5, 18]). In particular, we identify two types of SLOCC operators whose action can in certain cases preserve the usefulness of the cluster state as a resource. The first type, which we call N-type operators, comprises those operators that preserve the relative norms of the computational basis states. The second type, called B-type operators, are those that preserve their orthogonality (i.e. are in a sense basis-preserving).

In particular, we show that when N-type operators act on alternating qubits in a 1D cluster state, the state remains a quasi-deterministic resource for single-qubit rotations. We refer to such 1D states as N–U–N chains. In contrast to the cluster state, the number of measurements required to implement an arbitrary single-qubit rotation with an N – U – N chain is random rather than fixed. Furthermore, the state exhibits non-zero spin-spin correlations that decay exponentially with distance. These properties are shared by other resources previously appearing in the literature [4, 10, 20, 20], notably those based on the so-called AKLT model [21, 22]. We also show how 1D N – U – N chains can be coupled together to produce a quasi-deterministic 2D resource for universal MBQC.

Next, we show that when B-type operators act on alternating qubits in a 1D cluster state, the result is in general a probabilistic resource for single-qubit rotations. We call these states B – U – B chains. We find that under a restricted subset of B-type operators, the three-dimensional analogs of B – U – B chains constitute quasi-deterministic resources for MBQC under strictly projective measurements. A similar result was exhibited in Ref. [15], in which a 2D cluster state deformed by B-type operators was shown to be reducible to a percolated 2D cluster state [23] by the action of three-element POVMs. The B – U – B states have the interesting property that each qubit can be arbitrarily locally pure, or alternatively that an individual qubit can be arbitrarily weakly entangled with the rest of the state, as measured by the von Neumann entropy of entanglement. Like the cluster states, they also exhibit vanishing long-range correlations, with no spin-spin correlation functions beyond second-nearest-neighbor surviving.

The structure of the paper is as follows: in Section II, we briefly review the theory of measurement-based quantum computation using cluster states, and introduce the various definitions and notation used in the technical part of this paper. In Section III, we describe the effects of invertible local operators acting on a cluster state on the class of linear transformations that can be logically implemented via adaptive single-qubit measurements on this new state, and outline some strategies for dealing with these effects. In Section IV, we provide explicit examples of some structures of SLOCC-transformed cluster states that are universal for either probabilistic or deterministic single-qubit rotations or full MBQC. Finally, in Section V, we discuss the relationship of our resource states

with previously known quasi-deterministic resources, and outline the prospects of identifying hitherto unknown resource states by this method.

II. BACKGROUND

An n -qubit cluster state can be defined in terms of the stabilizer formalism [24] as the unique n -qubit pure state $|\text{Cl}_n\rangle$ satisfying the n conditions

$$X_i \bigotimes_{j \in \mathcal{N}(i)} Z_j |\text{Cl}_n\rangle = |\text{Cl}_n\rangle, \quad (2)$$

where $i \in \{1, \dots, n\}$ labels a qubit, $\mathcal{N}(i)$ denotes the spatial neighbourhood of qubit i , and X_i and Z_i denote the standard single-qubit Pauli operators, given in the computational basis by

$$X = \begin{bmatrix} 0 & 1 \\ 1 & 0 \end{bmatrix}; \\ Z = \begin{bmatrix} 1 & 0 \\ 0 & -1 \end{bmatrix},$$

acting on qubit i . Alternatively, the cluster state can be identified as the result of a dynamical process in which

1. n qubits are initialized in the state $|+\rangle^{\otimes n}$, where $|+\rangle \equiv \frac{1}{\sqrt{2}}(|0\rangle + |1\rangle)$ is the $+1$ -eigenstate of X ;
2. CZ entangling gates, whose action on the computational basis states is given by

$$\text{CZ}_{i,j}|x,y\rangle_{i,j} = (-1)^{x \cdot y} |x,y\rangle_{i,j}, \quad (3)$$

are applied between each pair of neighbouring qubits (i, j) . Thus,

$$|\text{Cl}_n\rangle = \prod_{\langle i,j \rangle} \text{CZ}_{i,j}|+\rangle^{\otimes n}, \quad (4)$$

where $\langle i, j \rangle$ indicates that i and j label neighbouring qubits.

For notational convenience, define a global entangling operation on a lattice,

$$\mathfrak{G}_{k,l} := \prod_{j=k}^{l-1} \text{CZ}_{j,j+1}, \quad (5)$$

to be the tensor product of CZ gates acting between all nearest-neighbour pairs of vertices on a line with labels between k and l . Now consider a modified one-dimensional n -qubit cluster state,

$$|\text{Cl}_n^{1D}\rangle' = \mathfrak{G}_{1,n}|\psi\rangle_1|+\rangle_{2,\dots,n}^{\otimes n-1}. \quad (6)$$

where the first qubit was encoded in some general pure state $|\psi\rangle$ before the global entangling operation $\mathfrak{G}_{1,n}$ was

performed. The effect of projectively measuring the first qubit, the one on which $|\psi\rangle$ was initially encoded, is to teleport the quantum information corresponding to the state $|\psi\rangle$ to the next qubit, subject to some linear transformation depending upon the basis and outcome of the measurement. To see this, assume that $|\psi\rangle = a|0\rangle + b|1\rangle$. We then find that

$$\begin{aligned} |\text{Cl}_n^{1D}\rangle' &= \mathfrak{G}_{2,n} \text{CZ}_{1,2} (a|0\rangle_{1,2} + b|1\rangle_{1,2}) |+\rangle_{3,\dots,n}^{\otimes n-2} \\ &= \mathfrak{G}_{2,n} (a|0\rangle_{1,2} + b|1\rangle_{1,2}) |+\rangle_{3,\dots,n}^{\otimes n-2} \\ &= \mathfrak{G}_{2,n} (a|0\rangle_1 \text{I}_2 + b|1\rangle_1 \text{Z}_2) |+\rangle_{2,\dots,n}^{\otimes n-1}. \end{aligned} \quad (7)$$

Projecting the first qubit via an arbitrary rank-1 projector $|m\rangle\langle m|$, the state of the system (neglecting the projected qubit and overall normalization) becomes

$$\begin{aligned} |\Phi\rangle &= \mathfrak{G}_{2,n} (a\langle m|0\rangle \text{I}_2 + b\langle m|1\rangle \text{Z}_2) |+\rangle_{2,\dots,n}^{\otimes n-1} \\ &= \mathfrak{G}_{2,n} (a\langle m|0\rangle |+\rangle_2 + b\langle m|1\rangle |-\rangle_2) |+\rangle_{3,\dots,n}^{\otimes n-2} \\ &= \mathfrak{G}_{2,n} \text{H}_2 (a\langle m|0\rangle |0\rangle_2 + b\langle m|1\rangle |1\rangle_2) |+\rangle_{3,\dots,n}^{\otimes n-2} \\ &\propto \mathfrak{G}_{2,n} \text{H}_2 (\langle m|+\rangle \text{I}_2 + \langle m|-\rangle \text{Z}_2) |\psi\rangle_2 |+\rangle_{3,\dots,n}^{\otimes n-2}, \end{aligned}$$

where the Hadamard operator $\text{H}_i = (\text{X}_i + \text{Z}_i)/\sqrt{2}$. In other words, the quantum information has been teleported to the second qubit through the linear transformation

$$\text{M} = \text{H} (\langle m|+\rangle \text{I} + \langle m|-\rangle \text{Z}). \quad (8)$$

Without loss of generality, the single-qubit state acting as the projector can be written as

$$|m(\xi, \phi)\rangle = \cos \frac{\xi}{2} |+\rangle + e^{i\phi} \sin \frac{\xi}{2} |-\rangle \quad (9)$$

for some $0 \leq \xi < 2\pi$, $-\pi \leq \phi < \pi$. Thus, the linear transformation through which the quantum information is teleported can be written as

$$\text{M} = \text{H} \left(\cos \frac{\xi}{2} \text{I} + e^{i\phi} \sin \frac{\xi}{2} \text{Z} \right). \quad (10)$$

In the special case that $\phi = \pm\pi$, corresponding to $|m\rangle$ lying on the $x-y$ plane of the Bloch sphere, this transformation becomes the (familiar from cluster state MBQC) unitary transformation $\text{HR}_z [\pm\xi]$. Thus, there is an entire single-parameter family of unitary gates through which the initial state $|\psi\rangle$ can be teleported, each corresponding to a projection of the first qubit on to some state lying in the $x-y$ plane. This family is universal for single-qubit rotations: via four projections, corresponding to $\xi = 0, \xi_2, \xi_3, \xi_4$ respectively, one teleports the transformation

$$\begin{aligned} \text{U}(\xi_2, \xi_3, \xi_4) &= \text{HR}_z [\xi_4] \text{HR}_z [\xi_3] \text{HR}_z [\xi_2] \text{HR}_z [0] \\ &= \text{R}_x [\xi_4] \text{R}_z [\xi_3] \text{R}_x [\xi_2], \end{aligned} \quad (11)$$

which is an arbitrary single-qubit unitary decomposed in terms of Euler angles.

To this point, we have not discussed how to compensate for the randomness associated with the measurements. If one were to drive the gate teleportation described above via projective measurements, measurements must be made in an orthonormal basis containing $|m(\xi, \phi = \pi)\rangle$. For a single qubit, this basis would be $\mathcal{B}(\xi, \phi) = \{|m(\xi, \phi)\rangle, |m^\perp(\xi, \phi)\rangle\}$, where

$$|m(\xi, \phi)\rangle = \cos \frac{\xi}{2} |+\rangle + e^{i\phi} \sin \frac{\xi}{2} |-\rangle; \quad (12)$$

$$|m^\perp(\xi, \phi)\rangle = \sin \frac{\xi}{2} |+\rangle - e^{i\phi} \cos \frac{\xi}{2} |-\rangle. \quad (13)$$

From Eq. (8), the teleported gate associated with the application of the projector $|m^\perp\rangle\langle m^\perp|$ on the first qubit would be

$$\begin{aligned} \text{M}^\perp &= \text{H} \left[\sin \frac{\xi}{2} \text{I} - e^{i\phi} \cos \frac{\xi}{2} \text{Z} \right] \\ &\equiv \text{XH} \left[\cos \frac{\xi}{2} \text{I} - e^{-i\phi} \sin \frac{\xi}{2} \text{Z} \right], \end{aligned}$$

where in the last step we have made use of the identity $\text{XH} = \text{HZ}$, and have dropped an unimportant overall phase. Once again considering the special case that $\phi = \pm\pi$, this reduces to

$$\text{M}^\perp = \text{XHR}_z [\pm\xi] = \text{XM}.$$

The teleported gate can be summarized succinctly as follows: measuring in the basis $\{|m\rangle, |m^\perp\rangle\}$ defined by Eqs. (12,13) with $\phi = \pi$, and denoting the measurement outcome by $m = 0$ for state $|m\rangle$ and $m = 1$ for $|m^\perp\rangle$, then the teleported gate is $\text{X}^m \text{HR}_z [\xi]$. The operator X can be thought of as a byproduct operator that occurs as a result of obtaining measurement outcome 1.

If the aim is to teleport the operator $\text{U}(\xi_2, \xi_3, \xi_4)$ defined in Eq. (11), then apparently one runs into a problem should a measurement outcome of 1 be obtained for any of the four measurements needed to teleport this gate. In fact the X byproduct operators can be pushed through the rotations because $\text{R}_z [\xi] \text{X} = \text{XR}_z [-\xi]$. Suppose then that one performs four projective measurements on a one-dimensional cluster state, with the i th measurement being a projective measurement of qubit i in the orthonormal basis $\mathcal{B}(\theta_i, \pi)$, $\theta_1 = 0$ and the measurement outcome denoted $m_i \in \{0, 1\}$. The quantum information originally situated on qubit 1 before the global entangling operation is then teleported through the gate

$$\begin{aligned} \text{M} &= \text{X}^{m_4} \text{HR}_z [\theta_4] \text{X}^{m_3} \text{HR}_z [\theta_3] \text{X}^{m_2} \text{HR}_z [\theta_2] \text{X}^{m_1} \text{H} \\ &= \text{X}^{m_4} \text{Z}^{m_3} \text{X}^{m_2} \text{Z}^{m_1} \text{R}_x \left[(-1)^{m_3+m_1} \theta_4 \right] \\ &\quad \times \text{R}_z [(-1)^{m_2} \theta_3] \text{R}_x [(-1)^{m_1} \theta_2]. \end{aligned} \quad (14)$$

Comparing Eq. (11) and Eq. (14), the choices $\theta_2 = (-1)^{m_1} \xi_2$, $\theta_3 = (-1)^{m_2} \xi_3$, and $\theta_4 = (-1)^{m_3+m_1} \xi_4$ make the implemented teleported gate

$$\text{M} = \text{X}^{m_4} \text{Z}^{m_3} \text{X}^{m_2} \text{Z}^{m_1} \text{U}(\xi_2, \xi_3, \xi_4). \quad (15)$$

Thus, any gate can be implemented by conditioning each of the last three measurement bases on the results of previous measurements, up to an overall Pauli byproduct operation. The byproduct is of no concern, as Z has no effect on computational basis states while X merely swaps them; this means that the effect of the byproduct can be taken into account simply by appropriate reinterpretation of the final measurement outcomes of the circuit, contingent on the intermediate measurement outcomes.

An equivalent description of this universal gate teleportation can be obtained within the Matrix-Product State (MPS) representation [4, 5] of the one-dimensional cluster state:

$$|\text{Cl}_n\rangle = \sum_{\vec{i}} A^{[1]}[i_1]A^{[2]}[i_2]\dots A^{[n]}[i_n]|i_1i_2\dots i_n\rangle, \quad (16)$$

where \vec{i} is an n -bit string and the site matrices $\{A^{[j]}[i_j]\}$ are all two-by-two, except for the boundaries; the $\{A^{[1]}[i_1]\}$ are row vectors and the $\{A^{[n]}[i_n]\}$ are column vectors. The site matrices are not unique, but it is particularly convenient if they are chosen to satisfy the relation $\sum_{i_j} A^{[j]}[i_j]A^{[j]\dagger}[i_j] = I$ for each j , corresponding to the canonical form of the MPS [25]. For the left and right boundaries one obtains $A^{[1]}[0] = \frac{1}{\sqrt{2}}\langle +|$, $A^{[1]}[1] = \frac{1}{\sqrt{2}}\langle -|$, $A^{[n]}[0] = |0\rangle$, and $A^{[n]}[1] = |1\rangle$; for the bulk sites $1 < j < n$ they are $A^{[j]}[0] = \frac{1}{\sqrt{2}}H$ and $A^{[j]}[1] = \frac{1}{\sqrt{2}}HZ = \frac{1}{\sqrt{2}}XH$. The ‘always-on’ operator H is teleported on each measurement of a qubit, and the X gate serves as the byproduct operator. In general, an MPS state is a universal resource for measurement-based single-qubit gate teleportation (a ‘computational wire’) if the bulk site matrices can be chosen to be proportional to unitaries [18]. In this case they can be written as $A^{[j]}[0] = \frac{1}{\sqrt{2}}W$ and $A^{[j]}[1] = \frac{1}{\sqrt{2}}WR_z(\phi)$ with $W \in SU(2)$ and $\phi \in \mathbb{R}$.

In the context of the calculations presented in the next two sections, it is worth pointing out that there are two special features associated with the projective single-qubit measurements on one-dimensional cluster states presented above. The first is that the linear transformation M on the quantum state $|\psi\rangle$ is guaranteed to be unitary; in practice, this means that the effect of such a measurement is not dependent on the input state $|\psi\rangle$. If the linear transformation is not unitary (for example projections of the local system outside the $x - y$ plane, as discussed below), then there is an equivalent unitary transformation resulting in the same final state vector; however, the equivalent unitary will depend on $|\psi\rangle$. The second feature is that the byproduct operator resulting from measurement outcome 1 is always X . This is beneficial as X operators can be pushed through R_z operators with an easily characterized effect, as discussed above. These properties can be summarized as follows:

- **Property IA:** the teleported gate is in general of the form $\text{HR}_z[\xi]$ where $\xi \in \mathbb{R}$, i.e. a unitary gate

corresponding to a z -axis rotation by a real angle, followed by a Hadamard gate.

- **Property IIA:** the byproduct operator is always $X \equiv R_x[\pi]$.

The above two features do not hold for single-qubit projective measurements outside the $x - y$ plane. In general,

- **Property IB:** the teleported gate is in general of the form $\text{HR}_z[\xi]$ where $\xi \in \mathbb{C}$, i.e. a non-unitary gate corresponding to a z -axis rotation by a complex angle, followed by a Hadamard gate.
- **Property IIB:** the byproduct operator is in general $R_x[\eta]$ where $\eta \neq \pi$ in general, i.e. an x -axis rotation not corresponding simply to Pauli X .

Another way to view this is that in $x - y$ plane, one always teleports $\text{HR}_z[\xi + \delta_{m,1}\pi]$ with $\xi \in \mathbb{R}$, whereas in any other plane, one teleports $\text{HR}_z[\xi + \delta_{m,1}\epsilon]$ where $\xi \in \mathbb{R}$ corresponds to the angle of the z -rotation in the desired gate, and $\epsilon \in \mathbb{C}$ is a complex error that occurs on measurement outcome 1.

Single-qubit gates alone are not sufficient for universal computation; at least one multiqubit entangling gate is required as well. In the cluster state model, multiqubit gates are accomplished via measurement patterns on 2D structures. Logical qubits are processed by horizontal 1D wires, while entangling operations are mediated by vertical links between them. An entangling gate that is locally equivalent to controlled-NOT can be achieved by measuring a link qubit in the Y basis [1, 2].

As with the case of single-qubit rotations, local Pauli byproduct operators may exist as well, depending on the measurement outcomes. As before, these byproduct operators are of no concern computationally. Thus there exists for cluster states a measurement pattern that deterministically implements a two-qubit unitary entangling gate, with any byproducts that occur being of the local Pauli type. It is not immediately clear that this will be the case for states other than the cluster state; in general, the teleported two-qubit gate may be non-unitary and the byproduct may be non-local. Any candidate resource state for MBQC must be shown to be amenable to a measurement pattern implementing some suitable two-qubit entangling gate. In Section III, we describe some 1D structures that are resources for single-qubit rotations and then in the examples of Section IV, we demonstrate how to perform entangling gates with natural 2D or 3D extensions of the 1D structures, and how to compensate the randomness associated the measurements.

III. PROJECTIVE MEASUREMENTS ON SLOCC-TRANSFORMED CLUSTER STATES

As discussed in the previous section, the distinguishing feature of MBQC with regular cluster states is that there

exists a plane of the Bloch sphere onto which successive, adaptive, single-qubit projective measurements drive an arbitrary computation that is deterministic and of fixed length. No matter which single-qubit gate is desired, it will be implemented with certainty up to an unimportant Pauli byproduct with four measurements. For an SLOCC-transformed cluster state, it is not obvious that there exists any such plane: in general it is not possible to simultaneously satisfy both Properties IA and IIA (or for the latter any another convenient Clifford gate). A natural question to ask is then: under what circumstances can either property IA or IIA be satisfied by itself? And if only one property is satisfied, does there remain a deterministic protocol for universal quantum computation? Sec. III A and Sec. III B discuss the circumstances under which it is possible to independently satisfy Property IA and IIA, respectively.

A. Strategy I: Guaranteed Unitary Evolution

1. Derivation of N -type Operators

For convenience, define

$$\mathbf{S}_{k,l} := \bigotimes_{j=k}^l S_j^{(j)} \quad (17)$$

where $S^{(j)} \in \text{GL}(2, \mathbb{C})$. From Eq. (7), it is clear that the SLOCC-transformed cluster state encoding quantum information can be written in the form

$$\mathbf{S}_{1,n} |\text{Cl}_n\rangle' = \mathbf{S}_{2,n} \mathfrak{G}_{2,n} \left(a S_1^{(1)} |0\rangle_1 \mathbf{I}_2 + b S_1^{(1)} |1\rangle_1 \mathbf{Z}_2 \right) |+\rangle_{2,\dots,n}^{\otimes n-1}. \quad (18)$$

Following the procedure discussed in Sec. II, applying the projector $|m\rangle\langle m|$ to the first qubit yields the resulting state on the remaining qubits:

$$\begin{aligned} |\Phi\rangle &= \mathbf{S}_{2,n} \mathfrak{G}_{2,n} \left(a \langle m | S_1^{(1)} |0\rangle \mathbf{I}_2 + b \langle m | S_1^{(1)} |1\rangle \mathbf{Z}_2 \right) |+\rangle_{2,\dots,n}^{\otimes n-1} \\ &= \mathbf{S}_{2,n} \mathfrak{G}_{2,n} \mathbf{H}_2 \mathbf{M}_2 |\psi\rangle_2 |+\rangle_{3,\dots,n}^{\otimes n-2}, \end{aligned}$$

where

$$\mathbf{M}_2 = \mathbf{H}_2 \left[\frac{\langle m | S^{(1)} |+\rangle}{\sqrt{2}} \mathbf{I}_2 + \frac{\langle m | S^{(1)} |-\rangle}{\sqrt{2}} \mathbf{Z}_2 \right]. \quad (19)$$

The only way for this to correspond to a unitary gate is if

$$\begin{aligned} \frac{1}{\sqrt{2}} \langle m | S^{(1)} |+\rangle &= e^{i\alpha} \cos \frac{\xi}{2}; \\ \frac{1}{\sqrt{2}} \langle m | S^{(1)} |-\rangle &= -i e^{i\alpha} \sin \frac{\xi}{2}, \end{aligned}$$

where $0 \leq \xi < 2\pi$, and therefore

$$S^{(1)\dagger} |m\rangle = \sqrt{2} e^{-i\alpha} \left[\cos \frac{\xi}{2} |+\rangle + i \sin \frac{\xi}{2} |-\rangle \right], \quad (20)$$

or equivalently

$$\begin{aligned} |m\rangle &= \sqrt{2} \left(S^{(1)\dagger} \right)^{-1} e^{-i\alpha} \left[\cos \frac{\xi}{2} |+\rangle + i \sin \frac{\xi}{2} |-\rangle \right] \\ &= e^{-i\alpha} \left(S^{(1)\dagger} \right)^{-1} \mathbf{R}_z [\xi] |+\rangle. \end{aligned} \quad (21)$$

Eq. (21) is the condition on the state $|m\rangle$ such that measurement outcome 0 yields a unitary teleported gate. Note that there is a family of states characterized by a single parameter ξ fulfilling this condition, not including the unimportant overall phase α .

To ensure that the measurement yields a unitary teleported gate independent of the measurement outcome, a similar condition must follow for the orthogonal complement $|m^\perp\rangle$. Orthogonality requires

$$\langle m^\perp | \propto \langle - | \mathbf{R}_z [-\xi] S^{(1)\dagger}, \quad (22)$$

and therefore

$$|m^\perp\rangle = c S^{(1)} \mathbf{R}_z [\xi] |-\rangle \quad (23)$$

for some constant $c \in \mathbb{C}$. Repeating the procedure that led to Eq. (20), but with $|m^\perp\rangle$ instead of $|m\rangle$, one obtains

$$S^{(1)\dagger} |m^\perp\rangle = \sqrt{2} e^{-i\beta} \left[\cos \frac{\xi}{2} |+\rangle + i \sin \frac{\xi}{2} |-\rangle \right]. \quad (24)$$

Substituting Eq. (23) into Eq. (24) yields

$$\begin{aligned} \sqrt{2} e^{-i\beta} \left[\cos \frac{\xi}{2} |+\rangle + i \sin \frac{\xi}{2} |-\rangle \right] &= c S^{(1)\dagger} S^{(1)} \mathbf{R}_z [\xi] |-\rangle \\ &= c S^{(1)\dagger} S^{(1)} \left[\cos \left(\frac{\xi}{2} \right) |-\rangle - i \sin \left(\frac{\xi}{2} \right) |+\rangle \right]. \end{aligned} \quad (25)$$

Rewriting Eq. (25) in the computational basis results in the expression

$$|0\rangle + e^{-i\xi} |1\rangle = c' S^{(1)\dagger} S^{(1)} (|0\rangle - e^{i\xi} |1\rangle) \quad (26)$$

for a suitably defined constant c' . Defining $T_k := S^{(k)\dagger} S^{(k)}$ and $T_k^{i,j} := \langle i | T_k | j \rangle$, we can see from Eq. (26) that

$$c' \left(T_1^{0,0} - e^{i\xi} T_1^{0,1} \right) = 1; \quad (27)$$

$$c' \left(T_1^{1,0} - e^{i\xi} T_1^{1,1} \right) = e^{-i\xi}. \quad (28)$$

From here, it is easily deduced that

$$\left| T_1^{0,0} - e^{i\xi} T_1^{0,1} \right| = \left| T_1^{1,1} - e^{-i\xi} T_1^{1,0} \right|. \quad (29)$$

Making use of the Hermiticity of T_k , simple algebra yields

$$T_1^{0,0} = T_1^{1,1}. \quad (30)$$

Eq. (30) above has a very simple geometric interpretation: it means that $S^{(1)}$ must preserve the relative norm

of the computational basis states. There is no requirement for $S^{(1)}$ to preserve their orthogonality, however, which means that $S^{(1)}$ is allowed to differ quite drastically from a unitary transformation; in fact, it can be made arbitrarily close to singular, as the relative angle between the computational basis states under the transformation by $S^{(1)}$ can be vanishingly small. We will refer to operators obeying this norm-preservation restriction as N-type operators.

Definition III.1. *A $GL(2, \mathbb{C})$ operator S satisfying $\langle 0|S^\dagger S|0\rangle = \langle 1|S^\dagger S|1\rangle$ is called an N-type operator.*

The singular value decomposition is helpful for characterizing N-type operators. An arbitrary SLOCC operator S can be written in terms of its singular value decomposition as $S = UDV$, where U is an arbitrary two-qubit unitary, D is a positive-definite diagonal matrix

$$D = \kappa \begin{bmatrix} \cos \theta & 0 \\ 0 & \sin \theta \end{bmatrix}, \quad (31)$$

where $0 < \theta < \frac{\pi}{2}$, and V is an arbitrary unitary matrix parametrized via the Euler decomposition as $V = HR_z[\alpha]R_x[\beta]R_z[\gamma]$, $0 \leq \alpha, \beta, \gamma < 2\pi$, and any global phase has been absorbed into U . It is then straightforward to determine that

$$\langle 0|S^\dagger S|0\rangle = \frac{1}{2}\kappa^2(1 + \cos 2\theta \sin \alpha \sin \beta); \quad (32)$$

$$\langle 1|S^\dagger S|1\rangle = \frac{1}{2}\kappa^2(1 - \cos 2\theta \sin \alpha \sin \beta). \quad (33)$$

So, if S is an N-type operator, we must have $\theta = \frac{\pi}{4}$ (in which case S is proportional to a unitary), $\alpha = 0$ or $\beta = 0$. The case where $\beta = 0$ still allows us to assume $\alpha = 0$ without loss of generality. Doing so, the $R_x[\beta]$ operator can be commuted past the H to turn into a z -rotation, and then absorbed into U . Thus we have the following characterization of N-type operators.

Lemma III.2. *Every N-type operator S must either be proportional to a unitary operator, or of the form $S = UDV$, where U is an arbitrary two-by-two unitary operator, D is defined as in Eq. (31) and $V = HR_z[\gamma]$ with $0 \leq \gamma < 2\pi$.*

It is straightforward to obtain an expression for the byproduct angle μ' in the case of measurement outcome 1 in terms of the parameters θ , γ and ξ (recall that this is the degree of freedom in the measurement basis). Using Eq. (19), it can easily be checked that the teleported gate when $|m\rangle \propto (S^\dagger)^{-1}R_z[-\xi]H|0\rangle$ is $M = HR_z[\xi]$, and when $|m\rangle \propto SR_z[-\xi]H|1\rangle$ is $M^\perp = R_x[\mu']HR_z[\xi]$, where the byproduct angle μ' obeys

$$\tan \frac{\mu'}{2} = \frac{1 - \cos 2\theta \cos(\gamma - \xi)}{\cos 2\theta \sin(\gamma - \xi)}. \quad (34)$$

The probabilities of the two measurement outcomes can also be easily calculated in terms of the same parameters,

and are found to be

$$p(0) = \frac{1}{2}(1 + \cos 2\theta \cos 2\xi); \quad (35)$$

$$p(1) = \frac{1}{2}(1 - \cos 2\theta \cos 2\xi). \quad (36)$$

This differs from the case of gate teleportation with a perfect cluster state, where the two measurement probabilities are always exactly $\frac{1}{2}$. That said, the expected probability of obtaining a byproduct here, averaged over all ξ , is

$$\langle p(1) \rangle_\xi = \frac{1}{2}, \quad (37)$$

irrespective of θ . We can thus generically expect to obtain an unwanted byproduct operator that we must compensate on half of our single-qubit measurements. This point will be discussed in Sec. IV.

2. Properties of N-Transformed Cluster States

Cluster states locally transformed by N-type operators can exhibit remarkably different properties from perfect cluster states. Nevertheless, as will be shown later in Sec. IV B, they can under some circumstances serve as universal resources for MBQC of random length.

Consider for the moment the Schmidt decomposition of an n -qubit cluster state on some set of qubits \mathcal{V} with respect to a bipartition separating qubit k from the rest:

$$|Cl_n\rangle_{\mathcal{V}} = \frac{1}{\sqrt{2}}(|0\rangle_k |Cl_{n-1}\rangle_{\mathcal{V}\setminus k} + |1\rangle_k Z_{\mathcal{N}(k)} |Cl_{n-1}\rangle_{\mathcal{V}\setminus k}), \quad (38)$$

where $|Cl_{n-1}\rangle_{\mathcal{V}\setminus k}$ refers to the cluster state resulting from deleting qubit k and $Z_{\mathcal{N}(k)}$ is the tensor product of Z operators acting on all the neighbors of k . This can be checked by verifying that this state satisfies the stabilizer conditions (2). The Schmidt basis for the multiqubit component can be further decomposed if desired by the same technique. The equality of the Schmidt coefficients in Eq. (38) demonstrates that any individual qubit in a cluster state has a maximally mixed local reduced density matrix, or in other words that it is maximally entangled with the rest of the cluster with respect to the von Neumann entanglement entropy. Likewise, exactly one ebit of entanglement is shared across any bipartition of the cluster state.

One effect of N-type operators is to change the local reduced density matrices of individual qubits within the state. In the canonical representation, the site matrices of the MPS representation [cf. Eq. (16)] are $A^{[j]}[0] = \frac{1}{\sqrt{2}}W = HR_z[-(\gamma^{(j)} + 2\theta^{(j)})]$ and $A^{[j]}[1] = \frac{1}{\sqrt{2}}WR_z[4\theta^{(j)}]$, which are both unitary. This immediately implies that the channel having these matrices as Kraus operators is unital, and like the ordinary cluster state one ebit of entanglement is shared across any bipartition. That said, the entanglement between any given qubit and the rest of the system need not be unity.

Consider for example the local reduced density matrix of a qubit adjacent to an endpoint of a 1D cluster state with n qubits, numbered 1 to n from left to right. Singling out first qubit 2 and then qubit 3, this state can be written as

$$|Cl_n^{1D}\rangle_{1\dots n} = \frac{1}{\sqrt{2}} (|0\rangle_2|+\rangle_1 I_3 + |1\rangle_2|-\rangle_1 Z_3) |Cl_{n-2}^{1D}\rangle_{3\dots n}. \quad (39)$$

Now consider the action of an N-type operator, $N^{(2)} = DHR_z[\gamma]$ on qubit 2, where the leading U operator is dropped because it can be absorbed into the measurement basis. It is easy to check that

$$N^{(2)}|Cl_n^{1D}\rangle_{1\dots n} = \frac{1}{\sqrt{2}} (\cos\theta|0\rangle_2|\Phi\rangle - i\sin\theta|1\rangle_2|\Phi^\perp\rangle), \quad (40)$$

where $|\Phi\rangle$ and $|\Phi^\perp\rangle$ are γ -dependent states for qubits 1, 3, \dots , n such that $\langle\Phi|\Phi^\perp\rangle = 0$. Thus, Eq. (40) remains a Schmidt decomposition. The local reduced density matrix of qubit 2 is

$$\rho_2 = \begin{bmatrix} \cos^2\theta & 0 \\ 0 & \sin^2\theta \end{bmatrix},$$

revealing that qubit 2 is no longer maximally entangled with the rest of the state. A similar calculation can be performed for qubits further from the boundary, with qualitatively similar results.

Another property of these states is the long-range behavior of two-point correlation functions, those of the form $C_{i,j}(\mathcal{A}, \mathcal{B}) := \langle\mathcal{A}_i\mathcal{B}_j\rangle - \langle\mathcal{A}_i\rangle\langle\mathcal{B}_j\rangle$ for some operators \mathcal{A} and \mathcal{B} . Two-point correlation functions of large 1D cluster states with periodic boundary conditions can be efficiently calculated using the Matrix Product State (MPS) representation. For an n -qubit ring, calculation of the correlation functions amounts to taking traces of products of $n/4 \times 4$ -dimensional matrices. Consider therefore a 1D cluster state with periodic boundary conditions (i.e. a ring), with the operation $N^{(i)}$ acting on qubit i . For this state, calculations show that all two-point Pauli correlation functions vanish except for the second-nearest-neighbour correlation function $C_{i-1,i+1}(Z, Z) = \cos 2\theta \sin \gamma$. This is in contrast to the perfect cluster state with periodic boundary conditions, for which all two-point correlation functions identically vanish.

As another example, the relevance of which will become clear in Sec. IV A, consider a ring with an even number of qubits, with N acting on every alternate qubit; say, the ones with even labels. In this case, the magnitude of the same two-point correlation function between odd-numbered qubits decays exponentially:

$$|C_{1,2j+1}(Z, Z)| \sim \exp\left(-\frac{2j}{L}\right). \quad (41)$$

The length scale L depends on θ and γ . The same correlation function between pairs of qubits with at least one even label is zero. The numerically obtained behavior of

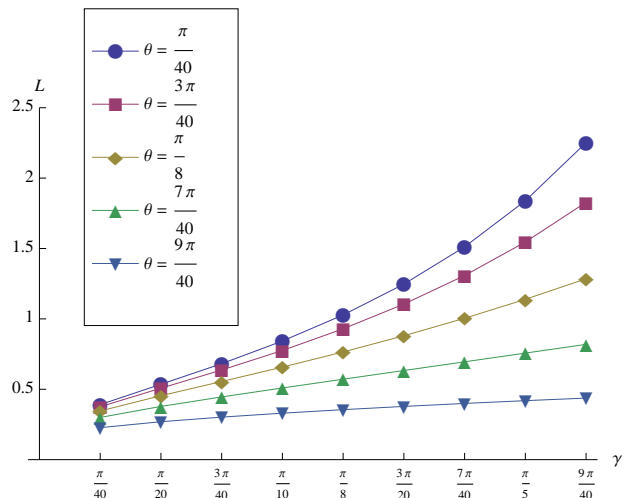


FIG. 1: (Color online) Correlation length scale L associated with the correlation function $|C_{1,2j+1}(Z, Z)| \sim \exp(-\frac{2j}{L})$ for a $N-U-N$ ring with all N-type operators identical, on a ring of 1000 qubits, as a function of the parameters of γ and θ , the parameters of N . The length scale increases as N approaches the singular limit, i.e. as θ gets close to 0 or $\pi/2$.

L for a ring of 1000 qubits is shown in Fig. 1 as a function of γ for several values of θ between 0 and $\pi/4$. As can be seen from the figure, the length scale increases with decreasing θ over this range, i.e. as the N-type operators approach the singular limit $\theta = 0$. The length scale is symmetric about $\theta = \pi/4$ between 0 and $\pi/2$. Viewed as a function of γ with θ held constant, the correlation function is convex and non-negative in γ over the interval from 0 to $\pi/2$ and is symmetric about $\pi/4$. For $\pi/2 \leq \gamma < \pi$, the magnitudes behave the same way as in the previous interval, but the signs alternate. The γ -behavior is periodic with period π . We note in passing that these non-zero correlation functions provides a lower bound for the localizable entanglement [26] between that pair of qubits in the state via projective measurements, with respect to the concurrence [27].

Note that a number of resources for MBQC with non-vanishing long-range correlation functions have been pointed out in the literature [5, 10, 13, 14, 20], based on the so-called spin-1 AKLT model [21, 22]. These states are quasi-deterministic resources, in the sense that measurement-based computations using these states can be made arbitrarily likely to succeed, either by reduction of the resource state to a deterministic resource or by a repeat-until-success strategy with each elementary gate requiring a random number of measurements. In Secs. IV A and IV B, we describe resource states called $N-U-N$ states that are based on cluster states transformed by N-type operators; these states share the properties of quasi-determinism and non-vanishing long-range correlations.

B. Strategy II: Guaranteed Pauli Byproduct

1. Derivation of B-Type Operators

Another possible strategy is to attempt to ensure that the byproduct operator is guaranteed to be Pauli-X, whether or not the teleported linear transformation is unitary. The advantage of this approach is that X has nice commutation properties through rotation operators about the z -axis, whether they be by real or complex angles, leading to the hope that the randomness inherent in the measurement process can be easily compensated.

When projectively measuring in the orthonormal basis $\{|m\rangle, |m^\perp\rangle\}$, the two possible operations that can occur are

$$M = H \left[\frac{\langle m|S^{(1)}|+\rangle}{\sqrt{2}} I + \frac{\langle m|S^{(1)}|-\rangle}{\sqrt{2}} Z \right]; \quad (42)$$

$$M^\perp = H \left[\frac{\langle m^\perp|S^{(1)}|+\rangle}{\sqrt{2}} I + \frac{\langle m^\perp|S^{(1)}|-\rangle}{\sqrt{2}} Z \right] \quad (43)$$

$$= XH \left[\frac{\langle m^\perp|S^{(1)}|-\rangle}{\sqrt{2}} I + \frac{\langle m^\perp|S^{(1)}|+\rangle}{\sqrt{2}} Z \right]. \quad (44)$$

Since I and Z are linearly independent, it follows that for the byproduct to be guaranteed to be proportional to Pauli-X, one must have

$$\langle m|S|+\rangle = c\langle m^\perp|S|-\rangle; \quad (45)$$

$$\langle m|S|-\rangle = c\langle m^\perp|S|+\rangle, \quad (46)$$

or equivalently,

$$\langle m|S|0\rangle = c\langle m^\perp|S|0\rangle; \quad (47)$$

$$\langle m|S|1\rangle = -c\langle m^\perp|S|1\rangle, \quad (48)$$

for some non-zero constant $c \in \mathbb{C}$. Suppose $S = UDV$ where U is an arbitrary single-qubit unitary, D is defined in Eq. (31), and $V = R_z[\beta]R_x[\gamma]R_z[\delta]$. Further suppose that $|m\rangle = UU'|0\rangle$ and $|m^\perp\rangle = UU'|1\rangle$, with $U' = R_z[\beta']R_x[\gamma']R_z[\delta']$. The reason for the appearance of U in the definitions of $|m\rangle$ and $|m^\perp\rangle$ is to compensate for the appearance of U in the singular value decomposition of S . The only effect of the $R_z[\delta']$ operation is to multiply the teleported gate by a global phase, so we can choose $\delta' = 0$ in what follows without loss of generality (it remains a free parameter for the applied unitary U'). Having done so, Eqs. (47-48) can be rewritten as

$$\langle 0|Q|0\rangle = c\langle 1|Q|0\rangle; \quad (49)$$

$$\langle 0|Q|1\rangle = -c\langle 1|Q|1\rangle, \quad (50)$$

where we have defined

$$Q := (U')^\dagger DV \quad (51)$$

$$\begin{aligned} &= R_x[-\gamma']R_z[-\beta']DR_z[\beta]R_x[\gamma]R_z[\delta] \\ &= R_x[-\gamma']R_z[\beta-\beta']DR_x[\gamma]R_z[\delta] \\ &:= R_x[-\gamma']R_z[b]DR_x[\gamma]R_z[\delta]; \end{aligned} \quad (52)$$

in the last line above we have defined $b := \beta - \beta'$. In the expression above, γ' and b are free parameters, while D , γ and δ are determined by the SLOCC operator S .

Return now to the constraints, Eqs. (49-50). Denoting $Q_{ij} := \langle i|Q|j\rangle$, one finds that $Q_{00}/Q_{10} = -Q_{01}/Q_{11}$. Note that neither Q_{10} nor Q_{11} can be zero; if either were zero, then the constraints would force Q and therefore S to be singular, which by assumption is not the case. This in turn means that

$$\text{Det}(Q) = 2Q_{00}Q_{11}. \quad (53)$$

From the definition of Q , Eq. (52),

$$\begin{aligned} \text{Det}(Q) &= \sin 2\theta; \\ 2Q_{00}Q_{11} &= \sin \gamma' \sin \gamma (\cos \gamma - i \cos 2\theta \sin b) \\ &\quad + \sin 2\theta (1 + \cos \gamma \cos \gamma'). \end{aligned} \quad (54)$$

Substituting the above expressions into Eq. (53) and equating real and imaginary parts gives us the two conditions

$$\sin \gamma' \sin \gamma \sin b \cos 2\theta = 0; \quad (55)$$

$$\cos \gamma (\sin \gamma' \sin \gamma + \cos \gamma' \sin 2\theta) = 0. \quad (56)$$

Recall that since S is invertible, we cannot have $\sin 2\theta = 0$ and since S is non-unitary, we cannot have $\cos 2\theta = 0$. The only ways to satisfy Eq. (55) are if $\sin \gamma' \sin \gamma = 0$ or $\sin b = 0$. In the first case, Eq. (56) immediately implies that $\cos \gamma' \cos \gamma = 0$, leaving b as a free parameter for our measurement basis. In the second case, γ' is fixed in terms of θ and γ , leaving no freedom in the measurement basis we are using. Furthermore, if we choose $\sin \gamma' = 0$, i.e. $\gamma' \in \{0, \pi\}$, then the measurement basis we are using is restricted to being the computational basis acted on by U (completely specified by S); again, no freedom. Therefore, the only solutions available to us that leave freedom in the measurement basis, and thus the teleported gate, are $\gamma \in \{0, \pi\}$ and $\gamma' \in \{\frac{\pi}{2}, \frac{3\pi}{2}\}$. Note that

$$S^\dagger S = \begin{bmatrix} 1 + \cos \gamma \cos 2\theta & -ie^{i\delta} \sin \gamma \cos 2\theta \\ ie^{-i\delta} \sin \gamma \cos 2\theta & 1 - \cos \gamma \cos 2\theta \end{bmatrix}. \quad (57)$$

Thus, demanding that the SLOCC operators allow for a guaranteed Pauli by-product, assuming the SLOCC operator is not unitary and thus $\cos 2\theta \neq 0$, is equivalent to demanding that $S^\dagger S$ be diagonal. Geometrically, this means that S must preserve the overlap of the computational basis states (the transformed computational basis is still orthogonal). We will refer to this kind of basis-preserving operator as a B-type operator.

Definition III.3. A $GL(2, \mathbb{C})$ operator S satisfying $\langle 0|S^\dagger S|1\rangle = \langle 1|S^\dagger S|0\rangle = 0$ is called a B-type operator.

A B-type operator can therefore be written

$$B = \begin{cases} UDR_z[\beta]R_z[\delta], & \gamma = 0 \\ UDR_z[\beta]XR_z[\delta], & \gamma = \pi, \end{cases}$$

ignoring overall phases. The two possibilities above can be simplified and collapsed into one. First, note that $R_z[\beta]$ can be commuted past D and absorbed into U . Next, note that XD is itself a diagonal matrix that results from swapping the diagonal entries of D . This means that the case where $\gamma = \pi$ can be written instead as $U'D'R_z[\delta]$, where $U' = UR_z[\beta]X$ and $D' = XD$. Of course, $R_z[\delta]$ can also be absorbed into U' ; thus, a simple and completely general expression for a B-type operator is

$$B = UD. \quad (58)$$

The diagonal matrix D in the singular value decomposition can be expressed as

$$D \propto \text{diag}(\cos(\theta), \sin(\theta)) = \sqrt{\sin(\theta)\cos(\theta)}R_z[i \ln \cot(\theta)],$$

so that the B-type operator becomes

$$B \propto UR_z[i \ln \cot(\theta)]. \quad (59)$$

Because the unitary U can be absorbed directly into the measurement basis, one can interpret B-type operators as z -rotations by an imaginary angle, the value of which is related to the ratio of the singular values.

When the local operator is B-type, the single-parameter family of measurement bases satisfies $\gamma' \in \{\frac{\pi}{2}, \frac{3\pi}{2}\}$, and $\beta' \in [0, 2\pi)$ is a free parameter. When this family of bases is used, the byproduct operator associated with measurement outcome 1 is always Z (up to a global phase). The teleported linear transformation is no longer unitary, however; it takes the form of a rotation about the z -axis of the Bloch sphere by a complex angle, followed by a Hadamard operation. The real part of the angle is completely specified by the choice of measurement basis, via the free parameter β' . The imaginary part is purely a function of the ratio of the singular values of the local $GL(2, \mathbb{C})$ operator. Denoting the measurement outcome corresponding to $\gamma' = \frac{\pi}{2}$ by $m = 0$ and that for $\gamma' = \frac{3\pi}{2}$ by $m = 1$, the teleported gate is given (up to a global phase) by

$$M = X^m HR_z[\beta' + i \ln \cot \theta]. \quad (60)$$

2. Properties of B-Transformed Cluster States

Interpreting the B-type operators as z -rotations by imaginary angles provides a simple insight into the nature of B-transformed cluster states. The R_z operator commutes with all CZ gates, so one can push it all the way through to the $|+\rangle$ states in the definition of the cluster state, Eq. (4). Because $R_z(\xi)|+\rangle$ is an arbitrary single-qubit state, B-transformed cluster states are equivalent to applying CZ gates between qubits in arbitrary states (not including computational basis states, which would require singular B operators).

One might assume that B-transformed cluster states are equivalent to weighted cluster states [28–32], but this is not in fact the case. Weighted graph states are defined as $\prod_{(i,j)} CP(\varphi)_{i,j}|+\rangle^{\otimes n}$, where the controlled-phase entangling gate is $CP(\varphi) = \text{diag}(1, 1, 1, e^{i\varphi})$; the cluster-state edge weights are then given by $w_{ij} = \varphi_{ij}$. Consider the simplest counter-example of a three-qubit linear cluster state with the central qubit transformed by a B-type operator $B = DR_z[\gamma]$ with $D = \text{diag}(\cos \theta, \sin \theta)$. The eigenvalues of the local reduced density matrices are all $\{\frac{1}{2}(1 \pm \cos 2\theta)\}$. On the other hand, for a three-qubit 1D weighted graph state with edge weights φ_{12} and φ_{23} , the eigenvalues of the reduced density matrix are $\frac{1}{2}(1 \pm \cos \frac{\varphi_{12}}{2})$, $\frac{1}{2}(1 \pm \frac{1}{2} \cos \varphi_{12} \cos \varphi_{23})$, and $\frac{1}{2}(1 \pm \cos \frac{\varphi_{23}}{2})$ for qubits 1 through 3, respectively. If the weighted graph and the B-transformed cluster are LU-equivalent, there must be some choice of φ_{12} and φ_{23} such that the spectra of the reduced density matrices are the same in both cases. For qubits 1 and 3 this implies $\phi_{12} = \phi_{23} = 4\theta$. For qubit 2 one obtains $\frac{1}{2}(1 \pm \frac{1}{2} \cos 4\theta^2)$. This matches the corresponding spectrum for the B-transformed cluster only when $\theta = \pm \frac{\pi}{4}, \varphi = \pm \pi$, in which case both states are LU-equivalent to a perfect cluster.

Cluster states locally transformed by B-type operators also exhibit different properties from perfect cluster states. As with N-type operators, B-type operators change the local reduced density matrices of individual qubits within the state, as described in the following lemma.

Lemma III.4. *Let $|Cl_n\rangle_{\mathcal{V}}$ be an n -qubit cluster state on the set of qubits \mathcal{V} , with some subset $\mathcal{Q} \subseteq \mathcal{V}$ acted upon by B-type operators. In particular, suppose that for each qubit $i \in \mathcal{Q}$, the B-type operator acting is given by $B^{(i)} = D^{(i)}$ with $D^{(i)} = \sqrt{2} \text{diag}(\cos \theta^{(i)}, \sin \theta^{(i)})$. Then, the local reduced density matrix for any qubit $k \in \mathcal{V}$ is given by*

$$\rho_k = \cos^2 \theta^{(k)} |0\rangle\langle 0| + \sin^2 \theta^{(k)} |1\rangle\langle 1| + \left(\frac{1}{2} \sin 2\theta^{(k)} \prod_{j \in \mathcal{N}(k)} \cos 2\theta^{(j)} |0\rangle\langle 1| + \text{h.c.} \right),$$

where $\theta^{(k)} := \frac{\pi}{4}$ if $k \notin \mathcal{Q}$.

The lemma is easily proved by taking advantage of the expression (38) for the Schmidt decomposition of a cluster state with one subsystem being qubit k alone, and then calculating ρ_k directly. The calculation is done by expressing the cluster state as the action of controlled-Z gates acting on the product state $|+\rangle^{\otimes n}$, and then using the fact that the $D^{(i)}$ and controlled-Z gates are mutually commuting. A consequence of this lemma is that the reduced density matrix of a given qubit is maximally mixed if and only if the qubit itself and at least one of its neighbors are untouched by B-type operators. In general, qubits within B-transformed cluster states are not maximally entangled with the rest of the state; in fact,

they can be arbitrarily weakly entangled (with respect to the von Neumann entanglement entropy).

Consider now a ring of an even number of qubits, with identical B-type operators specified by $\theta^{(2k)} = \theta$ acting on the qubits with even labels. The significance of such a state will become clear in Example IV D. Two-point correlation functions can be calculated exactly for this state. The result is that the nearest-neighbor correlation functions $C_{2k,2k\pm 1}(Z, X) = \cos 2\theta$ and the next-nearest-neighbor correlation functions $C_{2k,2k\pm 2}(Z, Z) = C_{2k-1,2k+1}(X, X) = \cos^2(2\theta)$ are the only ones that are non-zero, while all the other two-point Pauli correlation functions are identically zero. Again, this differs from the perfect cluster state, where all correlation functions are zero.

Exact calculations on chains of up to 7 qubits with identical (but arbitrary) B-type operators $B_{2j} = DR_z[\gamma^{(2j)}]$ acting on even qubits $2j$ reveal that the non-zero Schmidt coefficients corresponding to any bipartition of the chain into two contiguous halves are $\{\cos \theta, \sin \theta\}$. The von Neumann entropy of entanglement is equal to the Shannon entropy of this list, and is generally less than one ebit. The MPS representation bears out this observation. In the canonical form the site matrices for the boundary qubits are

$$A^{[1]}[0] = \frac{1}{\sqrt{2}}(\cos \theta^{(2)}\langle 0| + \sin \theta^{(2)}\langle 1|); \quad (61)$$

$$A^{[1]}[1] = \frac{1}{\sqrt{2}}(\cos \theta^{(2)}\langle 0| - \sin \theta^{(2)}\langle 1|); \quad (62)$$

$$A^{[n]}[0] = |+\rangle; \quad A^{[n]}[1] = -|-\rangle, \quad (63)$$

those for the bulk even sites are

$$A^{[2j]}[0] = \begin{bmatrix} 0 & e^{-i\gamma^{(2j)}} \\ 0 & 0 \end{bmatrix}; \quad (64)$$

$$A^{[2j]}[1] = \begin{bmatrix} 0 & 0 \\ e^{i\gamma^{(2j)}} & 0 \end{bmatrix}, \quad (65)$$

and those for the bulk odd sites are

$$A^{[2j-1]}[0] = \begin{bmatrix} \cos \theta^{(2j)} & \sin \theta^{(2j)} \\ \cos \theta^{(2j)} & \sin \theta^{(2j)} \end{bmatrix}; \quad (66)$$

$$A^{[2j-1]}[1] = \begin{bmatrix} -\cos \theta^{(2j)} & \sin \theta^{(2j)} \\ \cos \theta^{(2j)} & -\sin \theta^{(2j)} \end{bmatrix}. \quad (67)$$

It's very easy to verify that the channels induced by the matrices on the odd sites are not unital in the sense given in Ref. [18], so a B – U – B chain is not a quantum wire.

Such a 1D state would appear not to be capable of reliably processing a single qubit. This is true, but a simple modification of the geometry from one to two dimensions yields a usable resource for random length computation. This will be elaborated upon in Example IV D.

IV. RANDOM LENGTH COMPUTATION

Neither Strategy I nor Strategy II discussed in the previous section directly offers a way to perform determin-

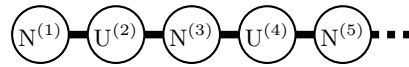


FIG. 2: N – U – N state, a one-dimensional structure that can be used for deterministic random-length single-qubit rotations.

istic single-qubit rotations. For Strategy I, it is unclear how to compensate for a byproduct operator $R_x[\eta]$ where $\eta \neq \pi$, as such a byproduct operator does not possess convenient commutation properties with the H and R_z operations. Similarly, for Strategy II, it is unclear whether some number of non-unitary teleported gates can be combined to form a desired unitary.

Another perspective on the strategies is that a single measurement with outcome 1 teleports the gate $HR_z[\xi + \epsilon]$, where $\xi \in \mathbb{C}$ is some angle associated with the always-on operation $HR_z[\xi]$ (in the terminology of Ref. [18]) and $\epsilon \in \mathbb{C}$ is a possibly complex error associated with the byproduct. To correct this error in principle requires two additional measurement steps. The first measurement step should teleport the gate $HR_z[0] \equiv H$, which would cancel the previously applied Hadamard gate; a possible X byproduct operator might result depending on the measurement outcome. On the second measurement step one would attempt to teleport $HR_z[-\epsilon]$ or $HR_z[\epsilon]$ depending on the previous measurement outcome, thus cancelling the original error ϵ .

This procedure is only possible if the measurement immediately after first incurring an error cannot itself generate any further error ϵ' . One way to guarantee such a circumstance is to impose that every alternate S_i operator is in fact unitary. Thus there must exist a class of states that are a strict subset of SLOCC-transformed cluster states, which constitute resources for random-length universal gate teleportation. Likewise, a subset of SLOCC-transformed cluster states in two dimensions must be universal resources for MBQC. The remainder of this section is devoted to various explicit examples.

A. Deterministic single-qubit rotations: N – U – N state

Consider a one-dimensional state of the form

$$|R\rangle = N_1^{(1)} \otimes U_2^{(2)} \otimes N_3^{(3)} \otimes U_4^{(4)} \dots \otimes N_n^{(n)} |Cl_n\rangle, \quad (68)$$

where the $\{N^{(i)}\}$ are N-type operators, and the $\{U^{(j)}\}$ are local unitaries (c.f. Fig. 2). The goal is to teleport the single-qubit unitary

$$U(\zeta, \eta, \xi) = R_x[\zeta] R_z[\eta] R_x[\xi]. \quad (69)$$

The first step is to use Strategy I to attempt a teleportation of $HR_z[0]$, analogously to the scheme with the perfect 1D cluster state. For the correct choice of basis the measurement outcome $m_1 = 0$ corresponds to success. One can then immediately measure qubit 2 in a

basis that teleports $X^{m_2}HR_z[\xi]$, and then use Strategy I to attempt the teleportation of $HR_z[(-1)^{m_2}\eta]$ starting on qubit 3.

If the first measurement outcome is instead $m_1 = 1$ then one instead teleports $HR_z[\epsilon]$ with $\epsilon \in \mathbb{R}$. This error must be immediately corrected, because the next desired rotation is around an orthogonal axis. Happily, there is a local unitary $U^{(2)}$ acting on the next qubit in the chain. The Hadamard operator that effects the now-undesired transformation of the rotation axes can be eliminated by teleporting another one ($H^2 = I$). This is accomplished by measuring the next qubit in the basis $\{U^{(2)}|+\rangle, U^{(2)}|-\rangle\}$. Labelling the measurement outcome m_2 , the teleported gates are

$$X^{m_2}HHR_z[\epsilon] \equiv X^{m_2}R_z[\epsilon]. \quad (70)$$

The measurement basis for qubit 3 is then chosen such that measurement outcome $m_3 = 0$ results in the gate $HR_z[(-1)^{m_2+1}\epsilon]$ being teleported. In this case, the overall unitary becomes

$$\begin{aligned} HR_z[(-1)^{m_2+1}\epsilon] X^{m_2}R_z[\epsilon] &= Z^{m_2}HR_z[-\epsilon]R_z[\epsilon] \\ &= Z^{m_2}H. \end{aligned}$$

At this point one has successfully teleported a Hadamard gate and an unimportant Pauli byproduct. The next measurement on a qubit with an even label can teleport the desired $HR_z[\xi]$ gate without error. One then attempts to teleport $HR_z[\eta]$ by measuring qubit 5, using Strategy I, etc.

The procedure corresponds to the following steps:

1. Measure qubit 1 with outcome m_1 in the basis

$$\left\{ (N^{(1)\dagger})^{-1}R_z[-\xi_1]H|0\rangle, N^{(1)}R_z[-\xi_1]H|1\rangle \right\}; \quad (71)$$

2. If $m_1 = 0$, then success;
3. If $m_1 = 1$ then one has effectively teleported the gate $R_x[\epsilon^{(1)}]HR_z[\xi_1]$, where

$$\epsilon^{(1)} = \pm 2 \arctan \frac{\cos 2\theta^{(1)} \cos \xi_1}{1 \pm \cos 2\theta^{(1)} \sin \xi_1} + \pi. \quad (72)$$

Note that $\epsilon^{(1)} = 0$ when $N^{(1)} = U^{(1)}$ ($\theta^{(1)} = \pi/4$), as expected. Measure qubit 2 with outcome m_2 in the basis $\{U^{(2)}X|0\rangle, U^{(2)}X|1\rangle\}$;

4. Measure qubit 3 with outcome m_3 in the basis $\{(N^{(3)\dagger})^{-1}R_z[\chi]H|0\rangle, N^{(3)}R_z[\chi]H|1\rangle\}$, where $\chi = (-1)^{m_2}\epsilon^{(1)}$;
5. Repeat steps 3 and 4 on successive qubits $2k$ and $2k+1$ until outcome 1 is achieved on an odd qubit, using $U^{(2)} \rightarrow U^{(2k)}$, $N^{(3)} \rightarrow N^{(2k+1)}$, $m_2 \rightarrow m_{2k}$, $\epsilon^{(1)} \rightarrow \epsilon^{(2k-1)}$.

The key point of this example is that as for any measurement on an odd-numbered qubit that yields the ‘correct’ outcome $m_i = 0$, one will have succeeded in implementing part of the desired single-qubit rotation. Furthermore, any errors resulting from outcomes $m_i = 1$ are correctible by making further measurements. This thus constitutes a repeat-until-success strategy, and gives rise to a quasi-deterministic random-length single-qubit rotation. The likely reason for this one-dimensional state to be capable of processing a logical qubit is that the left and right parts of the state share an ebit of entanglement with respect to any cut, as mentioned in Sec. III A 2.

B. Deterministic Universal MBQC: 2D N – U – N State

For universal MBQC, a two-dimensional resource state is required. The precise geometry of the two-dimensional state on which MBQC occurs is determined by the specific circuit to be implemented. Ideally one would start with a state defined on a convenient and simple geometry, and then ‘carve’ the desired shape out by deleting certain qubits. For cluster-state MBQC, for example, one carves the required state out of a rectangular lattice by projectively measuring the unwanted qubits in the computational basis. The goal is to yield isolated one-dimensional wires, each of which represents a logical qubit, with links only existing between wires in places where an entangling gate between logical qubits is needed.

Consider now a regular two-dimensional lattice composed of N – U – N states, as depicted in Fig. 3. As in the usual cluster state, logical qubits are processed by alternating horizontal wires composed of physical qubits, and entangling gates by vertical chains connecting them. Unlike the cluster case, however, the procedure for implementing single-qubit rotations with N – U – N states is of random length, so it is impossible to decide in advance where the desired links between wires will occur. The computational cluster state then must be carved ‘on the fly.’

Suppose that the quantum information encoding two logical qubits resides on (yet unmeasured) N-transformed physical qubits on two different wires. If an entangling gate between logical qubits is not desired at the next step, then the link between the wires can be first severed by measuring the intervening U-transformed chain qubit in the computational basis. An example of the method to decouple qubits 1 and 3 is shown in Fig. 3, where qubit 2 is measured in the computational basis. This has the effect of teleporting a Z gate to each of the logical qubits if the measurement outcome is $m = 1$. Other than taking into account the possible existence of these byproduct operators, the computation subsequently proceeds as in the one-dimensional case discussed above.

The desired entangling gate is implemented as follows. At the time that an entangling gate is needed, the local part of the resource state looks like two 1D N – U –

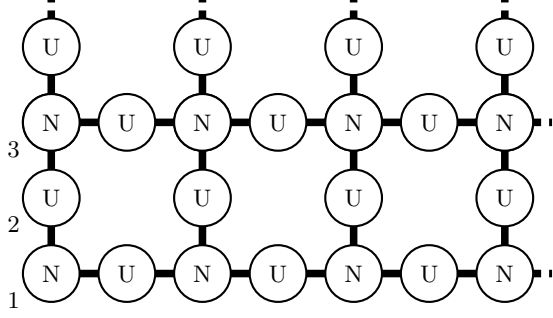


FIG. 3: 2D N – U – N state, universal for quasi-deterministic MBQC. The qubits labeled 1, 2 and 3 can be used to implement an entangling gate, which involves measuring qubit 2 in the Y basis. Alternatively, if an entangling gate is not desired here, qubits 1 and 3 can be decoupled by measuring qubit 2 in the Z basis.

N states, each coupled via CZ operations to an ancilla initially in the state $|+\rangle$ and subsequently acted on by an arbitrary U. In Fig. 3, the entangling link is represented by the vertical N – U – N chain labeled by qubits 1, 2, and 3. The local part of the state is mathematically described as

$$|R\rangle = N_1^{(1)}U_2^{(2)}N_3^{(3)}CZ_{1,2}CZ_{2,3}|c+t\rangle_{123}, \quad (73)$$

where the states $|c\rangle$ and $|t\rangle$ could be thought of as control and target states respectively for some entangling gate. Now, qubits 1 and 3 are measured in the usual Strategy I basis (71) with $\xi^{(i)} = 0$, while qubit 2 is measured in the eigenbasis of the Pauli operator Y, suitably rotated by $U^{(2)}$. This procedure teleports the state initially situated on qubits 1 and 3 through an entangling gate

$$G_{1,3} = R_x \left[\mu^{(1)} \right]_1^{m_1} X_1^{m_1+m_2} H_1 \\ \times R_x \left[\mu^{(3)} \right]_3^{m_3} X_3^{m_2+m_3} H_3 M_{1,3} \quad (74)$$

to qubits 4 and 5, with

$$M_{1,3} = |00\rangle\langle 00|_{1,3} + i|01\rangle\langle 01|_{1,3} + i|10\rangle\langle 10|_{1,3} + |11\rangle\langle 11|_{1,3}. \quad (75)$$

Here, the $\{\mu^{(i)}\}$ are the standard Strategy I byproduct angles, Eq. (34) or (72). This entangling operation is related to CZ via

$$CZ_{1,3} \equiv X_1 X_3 R_z[\pi/2]_1 R_z[\pi/2]_3 M_{1,3} X_1 X_3, \quad (76)$$

and so $G_{i,j}$ together with single-qubit operators forms a universal set of gates.

C. Probabilistic single-qubit rotations: B – U – B state

Next consider a one-dimensional state of the form

$$|R\rangle = B_1^{(1)} \otimes U_2^{(2)} \otimes B_3^{(3)} \otimes U_4^{(4)} \cdots \otimes B_{2n+1}^{(2n+1)} |Cl_{2n+1}\rangle, \quad (77)$$

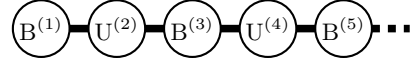


FIG. 4: B – U – B state, a one-dimensional structure that can be used for probabilistic random-length single-qubit rotations.

where the $\{B^{(2i+1)}\}$ are B-type operators, and the $\{U^{(2i)}\}$ are once again local unitaries (c.f. Fig. 4). This structure ensures that none of the bonds present in the structure is perfect; no particle has maximal entropy of entanglement with the rest of the state. This fact is a consequence of Lemma III.4; there is no qubit unaffected by B-type operators whose neighborhood contains any unaffected qubits.

All single-qubit measurements for the odd-numbered qubits now correspond to Strategy II, in which the byproduct operator is always X if it occurs. All even-numbered qubits are measured in the $\{U^{(2i)}|+\rangle, U^{(2i)}|-\rangle\}$ basis; as in the previous example, the only purpose of these measurements is to enable the removal of undesired contributions to the rotation angles. The main difference from the previous example is that a non-unitary gate of the form $HR_z[\xi_{2i+1}]$ is teleported, where $\xi_{2i+1} \in \mathbb{C}$. The present goal is therefore to compensate for the imaginary part of the rotation angle.

As discussed in the previous section and Eq. (60), the imaginary part of ξ_{2i+1} is entirely determined by the ratio of the singular values of $B^{(2i+1)}$, and can be defined as $\epsilon = i \ln(\cot \theta^{(2i+1)})$. Consider momentarily the special case where the $\{B^{(2i+1)}\}$ all have the same singular values. The gate teleported by a measurement of the B-transformed qubit $2i+1$ will then be proportional to $R_z[\epsilon(-1)^{m_{2i}+m_{2i-2}+\dots}]$, ignoring all rotations about real angles which are entirely determined by the choice of measurement basis. In short, the sign of the imaginary angle depends on the outcomes of the previous measurements on even-numbered U-transformed qubits.

The imaginary component therefore undergoes a random walk of step-length $|\epsilon|$. In particular, the walker takes its first step to the right when the first measurement outcome of an even-numbered qubit is 0, and to the left if it is 1. Subsequently, a measurement outcome of 0 on an even-numbered qubit causes the walker to take another step in the same direction as the previous step, while outcome 1 makes the walker take a step in the opposite direction.

The two possible measurement outcomes with odd qubits are always equally likely, but the probabilities with even qubits depend on the singular values of the B-type operators from the (odd) neighboring qubits, and generally speaking the walker is more likely to stray further from the origin than to step back towards it. For example, consider measuring the first two qubits of $|R\rangle$ in Eq. (77) in the $\{|+\rangle, |-\rangle\}$ basis. It can easily be shown, using the Schmidt decomposition (38) and the expression (58), that the probabilities of the outcome $|\pm\rangle$ on qubit 1 are equal, and that those on qubit 2 are

$$p_{\pm,2} = \frac{1}{2} \left(1 \pm \cos 2\theta^{(1)} \cos 2\theta^{(3)} \right). \quad (78)$$

Here, the random walk effectively begins at position $\ln(\tan \theta^{(1)})$ and moves to $\ln(\tan \theta^{(1)}) \pm \ln(\tan \theta^{(3)})$. For a situation to arise where the walker moves closer to the origin with probability greater than 1/2, one of the two pairs of conditions

$$\left| \ln(\tan \theta^{(1)}) \pm \ln(\tan \theta^{(3)}) \right| > 2 \left| \ln(\tan \theta^{(1)}) \right| \quad (79)$$

$$\pm \cos 2\theta^{(1)} \cos 2\theta^{(3)} > 0 \quad (80)$$

must be simultaneously satisfied, for either sign. If the $\{\theta^{(i)}\}$ are chosen uniformly at random, then the probability of this happening is only about 0.315. If this measurement procedure is continued down the chain, with qubits 3-5 relabelled 1-3 after the first two measurements and so on, the current value of $\theta^{(1)}$ tends to drift away from $\pi/4$ towards either 0 or $\pi/2$, and the range of values of $\theta^{(3)}$ for which the walker is likely to turn around and walk towards the origin progressively shrinks. Furthermore, if $\{\theta^{(1)}\}$ and $\{\theta^{(3)}\}$ are equal at any time, the walker is guaranteed to be more likely to continue in one direction than to turn around.

This procedure constitutes a probabilistic method for implementing a single-qubit rotation. Unfortunately if the walker strays too far from the origin, it becomes effectively impossible to recover and the attempted gate teleportation fails. The entire computation must then be repeated. If the singular values of the B^{2i+1} are chosen such that the imaginary components of the teleported angles are all integer multiples of each other, then the behavior of the random walk is even more deleterious. A judicious two-dimensional arrangement of B – U – B chains avoids this catastrophe, as discussed in the next example.

D. Universal MBQC: Percolated 2D Cluster State from 3D B – U – B state

In the previous example using Strategy II, a possibly infinite number of steps may be required to teleport an arbitrary single-qubit unitary. But quitting the protocol results in catastrophic failure: because the computational wire is effectively broken, the entire gate teleportation must be attempted from the beginning. A solution to these problems is to employ the 3D extension to the previous resource, corresponding to a cluster state transformed by alternating B-type operators and unitaries. This corresponds to a lattice with two interpenetrating cubic sublattices, a B-lattice and a U-lattice.

An example of this 3D resource, a cube with side length 3, is depicted in Fig. 5. Initially, Z-basis measurements in the z -direction (as labeled in Fig. 5) are used to carve out a structure in which each B-transformed qubit in the $x - y$ plane, shaded grey, is attached to a long vertical

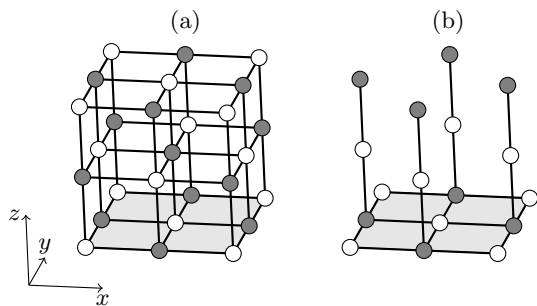


FIG. 5: 3D cluster state with B-type operators and unitaries acting on alternate qubits (a) before carving and (b) after carving. Grey qubits are acted upon by B-type operators and white qubits by local unitaries. Z-basis measurements are made in the z direction in (a) to disentangle those vertical chains originating from a white qubit in the $x - y$ plane. A measurement protocol along the remaining vertical chains in (b) produces a percolated 2D cluster in the $x - y$ plane.

B – U – B chain. Measurements are made on the chain qubits, starting at qubit above the B-transformed qubit on the computational wire and continuing in the vertical direction until success (defined below) is achieved. The goal is to probabilistically produce perfect entanglement in the $x - y$ plane, thereby effectively eliminating the B operators in the horizontal direction. The result is a 2D cluster state in this plane with missing entanglement bonds in random locations. As long as the mean density of broken links exceeds the percolation threshold for a two-dimensional square lattice, the resource is universal for MBQC [23].

Consider the first vertical chain from the left in Fig. 5. Recall that one can interpret B as a z -rotation by an imaginary angle $\pm i \ln \lambda$, as shown in Eq. (59). For simplicity, we assume the unitary operators acting on even-numbered qubits are all equal to the identity; were they not, they could be compensated by a suitable rotation of the measurement basis for. The portion of the state corresponding to the first four qubits of the vertical chain (with the qubit that intersects the horizontal chain labeled 1), is then (ignoring normalization)

$$\begin{aligned} |T\rangle &= B_1 B_3 C Z_{1,2} C Z_{2,3} C Z_{3,4} |++++\rangle_{1234} \\ &= R_z [i \ln \lambda]_1 R_z [i \ln \lambda]_3 |C1_4\rangle_{1234}, \end{aligned}$$

ignoring normalization factors as usual. First, qubits 2 and 3 are measured in the $\{|+\rangle, |-\rangle\}$ basis (of course, the measurement basis for qubit 2 would need to be rotated if a local unitary $U^{(2)}$ were acting). These are commuting measurements, since they are on different qubits and not adaptive. The effect is to teleport the state $R_z [i \ln \lambda] |+\rangle$ from qubit 3 through $X^{m_2} H X^{m_1} H \equiv X^{m_2} Z^{m_1}$ to qubit 1, yielding the new state

$$\begin{aligned} |T'\rangle &= R_z [i \ln \lambda]_1 C Z_{1,4} X_1^{m_2} Z_1^{m_1} R_z [i \ln \lambda]_1 |++\rangle_{14} \\ &= C Z_{1,4} R_z [i((-1)^{m_2} + 1) \ln \lambda]_1 |++\rangle_{14} \end{aligned}$$

up to overall local unitaries on the final state.

If $m_2 = 1$, then the imaginary part of the rotation angle is completely canceled. Qubit 4 can then be measured in the computational basis (again, suitably rotated if necessary) to disentangle the rest of the vertical chain from the horizontal chain. The result is a perfect cluster along the first three qubits in the horizontal direction, and the B-type operator is effectively deleted.

If $m_2 = 0$, then the situation is similar to the original. There is still a B-type operator present in the horizontal direction, now corresponding to a z-rotation about an angle with imaginary part $2\ln\lambda = \ln\lambda^2$. In other words, the new effective B-type operator in the horizontal chain has a ratio of singular values that is the square of the original one. In order to remove the effect of the B-type operator, the chain qubits must be measured sequentially until the total number of steps towards the origin exceeds by 1 the total number of steps away.

The probabilities $p_0^{(k)}$ and $p_1^{(k)}$ of the outcomes 0 and 1 on an even qubit in the vertical chain, where $k > 0$ is the present position of the walker on the real number line, are given by

$$p_0^{(k)} = \frac{1 + \lambda^{2k+2}}{1 + \lambda^2 + \lambda^{2k} + \lambda^{2k+2}} \sim O(1); \quad (81)$$

$$p_1^{(k)} = \frac{\lambda^2 + \lambda^{2k}}{1 + \lambda^2 + \lambda^{2k} + \lambda^{2k+2}} \sim O(\lambda^2). \quad (82)$$

The total probability p_n that the effect of the B will be undone within $2n$ measurements is the sum of the probabilities of all of the possible trajectories of the walker on n or fewer steps with initial position 1, final position 0 and all intermediate positions strictly positive.

The probability p_{10} of undoing the B operator after 10 attempts (20 measurements) is shown in Fig. 6 as a function of the ratio of singular values λ . Calculation of the exact probability p_∞ is computationally intractable, for two reasons. First, the number of valid trajectories for the walker grows exponentially in the number of steps allowed. Second, the probability of any particular trajectory depends on the full history of the walker, not just the number of steps. Of course, p_∞ must approach 1 as λ approaches unity (the limit that B becomes a unitary matrix). In this case, the walk reduces to the simple 1D random walk, which is known to sample the origin frequently.

If after some predetermined number of measurements along a vertical chain one has not yet succeeded in undoing B, the qubit at the root of the chain (i.e. in the computational wire) can be measured in the computational basis and thereby deleted. The result is a broken link in the 2D cluster state. The important result shown in Fig. 6 is that there is a critical value of λ , called λ_c , above which the probability of successfully undoing the B rises above the (bond) percolation threshold for a 2D square lattice (approximately 0.593). For this walk, the critical value obeys $\lambda_c \lesssim 0.379$. The upper bound for λ_c is read off the thick blue curve from Fig. 6. Thus, this procedure probabilistically yields a universal resource for

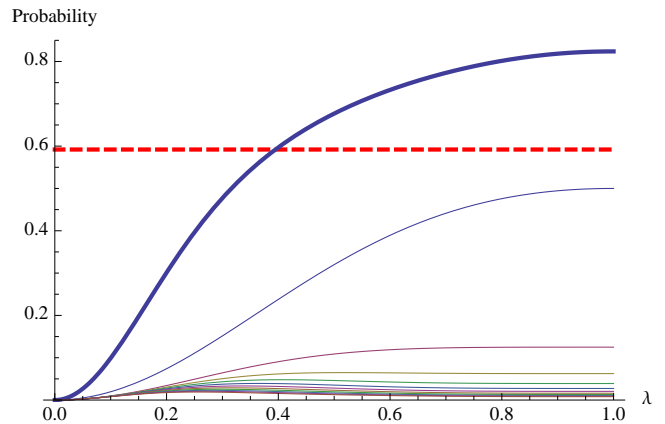


FIG. 6: (Color online) Probability of success of the procedure for deleting a B-type operator in the plane via a random walk in the third dimension, as a function of the ratio λ of the singular values (thick blue, color online). The probabilities p_k of deleting B with exactly k even-qubit measurements are also shown for k from 1 to 10 (thin, decreasing with increasing k), and the thick blue line is the sum of these. The red dashed line is the percolation threshold.

MBQC provided that λ is sufficiently large. We note that a similar example was considered in [15], where the resource was a 2D cluster state with identical B-type operators acting everywhere and the percolation proceeded via two-element POVMs that either removed the B or deleted the qubit. There, the critical value of λ was found to be 0.649.

V. DISCUSSION AND CONCLUSIONS

Motivated by a desire to identify new resource states for measurement-based quantum computing, we have performed a (non-exhaustive) search of the equivalence class of n -qubit cluster states on a rectangular lattice, under the action of $GL(2, \mathbb{C})^{\otimes n}$. In particular, our aim was to identify which states within this class could be used as resources for MBQC, by designing explicit protocols for teleporting single-qubit gates and two-qubit entangling gates, driven by adaptive local projective measurements. We identified a class of one-dimensional states, the so-called N – U – N states, that are deterministically universal for single-qubit rotations, although with a random number of measurements needed to teleport the desired rotation. We also identified a probabilistically universal resource for single-qubit rotations: the so-called B – U – B states. We then described a three-dimensional extension of B – U – B states that can yield a universal resource for deterministic MBQC beyond a percolation threshold, and a 2D N – U – N state that is also universal for deterministic but random-length MBQC.

Several interesting open issues arise as the result of this work. First, it is not clear what (if any) relationship exists between the states uncovered in this work and other

known resource states. For example, the probabilistic nature of the protocol with $B - U - B$ states has features in common with that of other resources for MBQC, such as photonic cluster states prepared via probabilistic entangling gates or with unreliable sources [33–36]. Likewise, the quasi-deterministic $N - U - N$ states share various characteristics with the AKLT-inspired resources of Refs. [5, 10, 15, 20], in particular the exponential spin correlations and the repeat-until-success measurement-based strategies. One distinction is that only one alternating sublattice of the $N - U - N$ states exhibits non-zero correlation functions, whereas in the AKLT chain, every qubit is correlated with every other. Presumably a true identification of an AKLT-type resource with a N -transformed cluster state will require N -type operators to be present on every qubit, a case we have not handled here.

Also, it will be important to better understand the relationships of these states with the universal quantum wires of Ref. [18]. In that work, certain reasonable physical assumptions were imposed on 1D wires at the outset, for example: the possibility of producing a wire via a translationally invariant nearest-neighbour global entangling operation, the asymptotic sharing of an ebit of entanglement between the left and right halves of the chain, etc. In our work, it is not clear if a translationally invariant scheme exists for producing $N - U - N$ or $B - U - B$ chains. Evidence from exact calculations on small chains and the explicit description of the states within the MPS representation reveals that although the left and right halves of $N - U - N$ chains share an ebit, the halves of the $B - U - B$ chains do not. This seems reasonable, as the $N - U - N$ chain is quasideterministically universal for single-qubit rotations, while the $B - U - B$ chain is only probabilistically so.

Second, it is conceivable that all states that have been hitherto identified as universal resources for MBQC are in fact SLOCC-equivalent to the family of cluster states. There is some evidence to support this conjecture. For example, the results of Ref. [19] show that many seemingly diverse resource states can be reduced to cluster states via local strategies. Similarly, the proof of the universality of the 2D AKLT state on a honeycomb lattice proceeds via local reduction to a random graph state, which can in turn be reduced to a percolated cluster state [14]. This reduction is successful despite the fact

that the initial resource is defined on qutrits rather than qubits, and on a non-rectangular lattice. An even more intriguing possibility (though we believe it to be unlikely) is that all possible states for universal MBQC fall within the SLOCC-equivalence class of the cluster states. At the very least, the relative size of this class decreases exponentially with the total number of physical qubits, as expected [16, 17].

Third, while we have shown that a certain subset of the orbit of the cluster states under SLOCC are useful resources, either probabilistically or quasi-deterministically, it is not clear if the remaining SLOCC-transformed cluster states are also universal resources for MBQC. Generically, single-qubit measurements on these states teleport gates with byproduct operators that are rotations about the X axis by complex angles. One possibility is that there is a measurement protocol that can accommodate all possible byproducts that we simply haven't found. Perhaps there is another sense, besides quasi-deterministic or probabilistic, in which these states can be said to be useful for MBQC. Another possibility is that there is some map from the full orbit to the particular subset of states considered in the work. Alternatively, the states in the full orbit may not be useful resources, though we have not attempted to prove this.

Finally, it would be useful if the resources presented in this work could be realized as the ground states of a physical Hamiltonian. A recent no-go theorem [37] shows this cannot be the case for frustration-free Hamiltonians on qubits. The question remains open for frustrated Hamiltonians, for instance the AKLT Hamiltonian in the Haldane phase [20–22]. Another possibility is that the ground states of physical Hamiltonians could be locally reduced to the resources we have found. Further research is needed to answer these and related questions.

VI. ACKNOWLEDGEMENTS

The authors are grateful to Jens Eisert, David Gross, and Gilad Gour for stimulating discussions. This research was supported by Alberta Innovates - Technology Futures and the Natural Sciences and Engineering Research Council of Canada (NSERC).

-
- [1] R. Raussendorf and H. J. Briegel, *Phys. Rev. Lett.* **86**, 5188 (2001).
 - [2] R. Raussendorf, D. E. Browne, and H. J. Briegel, *Phys. Rev. A* **68**, 022312 (2003).
 - [3] M. Van den Nest, W. Dür, A. Miyake, and H. J. Briegel, *New J. Phys.* **9**, 204 (2007).
 - [4] D. Gross and J. Eisert, *Phys. Rev. Lett.* **98**, 220503 (2007).
 - [5] D. Gross, J. Eisert, N. Schuch, and D. Perez-Garcia, *Phys. Rev. A* **76**, 052315 (2007).
 - [6] G. Gour and N. R. Wallach, *J. Math. Phys.* **51**, 112201 (2010).
 - [7] M. A. Nielsen, *Rep. Math. Phys.* **57**, 147 (2006).
 - [8] M. Van den Nest, K. Luttmer, W. Dür, and H. J. Briegel, *Phys. Rev. A* **77**, 012301 (2008).
 - [9] S. D. Bartlett and T. Rudolph, *Phys. Rev. A* **74**, 040302(R) (2006).
 - [10] G. K. Brennen and A. Miyake, *Phys. Rev. Lett.* **101**,

- 010502 (2008).
- [11] X. Chen, B. Zeng, Z.-C. Gu, B. Yoshida, and I. L. Chuang, *Phys. Rev. Lett.* **102**, 220501 (2009).
- [12] A. C. Doherty and S. D. Bartlett, *Phys. Rev. Lett.* **103**, 020506 (2009).
- [13] A. Miyake, *Phys. Rev. Lett.* **105**, 040501 (2010).
- [14] T.-C. Wei, I. Affleck, and R. Raussendorf, *Phys. Rev. Lett.* **106**, 070501 (2011).
- [15] C. E. Mora, M. Piani, A. Miyake, M. Van den Nest, W. Dür, and H. J. Briegel, *Phys. Rev. A* **81**, 042315 (2010).
- [16] D. Gross, S. T. Flammia, and J. Eisert, *Phys. Rev. Lett.* **102**, 190501 (2009).
- [17] M. J. Bremner, C. Mora, and A. Winter, *Phys. Rev. Lett.* **102**, 190502 (2009).
- [18] D. Gross and J. Eisert, *Phys. Rev. A* **82**, 040303 (2010).
- [19] X. Chen, R. Duan, Z. Ji, and B. Zeng, *Phys. Rev. Lett.* **105**, 020502 (2010).
- [20] S. D. Bartlett, G. K. Brennen, A. Miyake, and J. M. Renes, *Phys. Rev. Lett.* **105**, 110502 (2010).
- [21] I. Affleck, T. Kennedy, E. H. Lieb, and H. Tasaki, *Phys. Rev. Lett.* **59**, 799 (1987), ISSN 0031-9007.
- [22] I. Affleck, T. Kennedy, E. H. Lieb, and H. Tasaki, *Comm. Math. Phys.* **115**, 477 (1988), ISSN 0010-3616.
- [23] K. Kieling, T. Rudolph, and J. Eisert, *Phys. Rev. Lett.* **99**, 130501 (2007).
- [24] D. Gottesman, Ph.D. thesis, California Institute of Technology (1997).
- [25] D. Perez-Garcia, F. Verstraete, M. M. Wolf, and J. I. Cirac, *Quant. Inf. Comput.* **7**, 401 (2007).
- [26] M. Popp, F. Verstraete, M. A. Martín-Delgado, and J. I. Cirac, *Phys. Rev. A* **71**, 042306 (2005).
- [27] W. K. Wootters, *Quant. Inf. Comput.* **1**, 27 (2001).
- [28] W. Dür, L. Hartmann, M. Hein, M. Lewenstein, and H.-J. Briegel, *Phys. Rev. Lett.* **94**, 097203 (2005).
- [29] J. Calsamiglia, L. Hartmann, W. Dür, and H.-J. Briegel, *Phys. Rev. Lett.* **95**, 180502 (2005).
- [30] S. Anders, M. B. Plenio, W. Dür, F. Verstraete, and H.-J. Briegel, *Phys. Rev. Lett.* **97**, 107206 (2006).
- [31] M. Hein, W. Dür, J. Eisert, R. Raussendorf, M. Van den Nest, and H. J. Briegel, in *International School of Physics Enrico Fermi (Varenna, Italy), Quantum computers, algorithms and chaos*, edited by P. Zoller, G. Casati, D. Shepelyansky, and G. Benent (2006).
- [32] S. Anders, H. J. Briegel, and W. Dür, *New Journal of Physics* **9**, 361 (2007).
- [33] D. Gross, K. Kieling, and J. Eisert, *Phys. Rev. A* **74**, 042343 (2006).
- [34] K. Kieling, D. Gross, and J. Eisert, *J. Opt. Soc. Am. B* **24**, 184 (2007).
- [35] K. Kieling, D. Gross, and J. Eisert, *New J. Phys.* **9**, 200 (2007).
- [36] K. Kieling, J. L. O'Brien, and J. Eisert, *New J. Phys.* **12**, 013003 (2010).
- [37] J. Chen, X. Chen, R. Duan, Z. Ji, and B. Zeng, *Phys. Rev. A* **83**, 050301 (2011).